Circular in situ neutron powder diffraction cell for study of reaction mechanism in electrode materials for Li-ion batteries

Vikram Godbole, Michael Hess, Claire Villevieille, Hermann Kaiser, Jean-François Colin, Petr Novak

RSC Advances

RSC Publishing

PAPER

View Article Online
View Journal | View Issue

Circular *in situ* neutron powder diffraction cell for study of reaction mechanism in electrode materials for Li-ion batteries†

Cite this: *RSC Advances*, 2013, **3**, 757

Vikram A. Godbole,‡ Michael Heß, Claire Villevieille, Hermann Kaiser, Jean-François Colin§ and Petr Novák*

The study of reaction mechanisms in materials for Li-ion batteries mainly involves localization of lighter elements like Li, O, or even H in the structure. Thus, in order to facilitate *in situ* localization of lighter elements and *in situ* study of structural evolution in the electrode materials, a circular *in situ* neutron diffraction cell capable of cycling small amounts of electrode materials (0.2–0.3 g) was developed for primary use at the D20 beamline at ILL, Grenoble, France. The circular cell design was tested using $LiFePO_4$ and graphite as the model electrode materials. The effect of using deuterated electrolyte *versus* protonated electrolyte on the quality of the *in situ* neutron diffraction data was also investigated. First *in situ* neutron powder diffraction measurements at ILL, Grenoble, were successfully conducted where each neutron diffraction pattern was recorded in only 24 min, delivering very good time resolution. It was also found that a circular cell design holding only a small amount of material soaked in deuterated electrolyte was best to perform quantitative analysis using the Rietveld method over the complete 2 theta range. The pattern shows no apparent anisotropic absorption of the diffracted neutron beams.

Received 23rd July 2012,
Accepted 7th November 2012

DOI: 10.1039/c2ra21526h

www.rsc.org/advances

Introduction

Portable power sources have undergone a rapid evolution in the last decade, leading to smaller and more efficient devices for various applications ranging from personal electronic devices to hybrid vehicles. Among these, lithium-ion batteries are prominent for their ability to deliver both high power and high energy density.[1] Lithium-ion batteries work on the following principle: both anode and cathode are based on host materials (often layered structures) allowing reversible reaction with lithium ions.[2] Understanding the structural changes in these intercalation, insertion, or alloy materials during lithiation/delithiation is an important prerequisite for their further development. An excellent method for studying the structural changes in these materials during electrochemical cycling is the use of Bragg diffraction (X-ray and neutrons).

The differences in the scattering of X-rays and neutrons by atoms/nuclei are of great interest for electrode materials. Most of the studies of reaction mechanisms involve localizing lighter elements like Li, H, or O in the structure. These elements are essentially non-scattering to X-rays, however they show higher scattering to neutrons and hence can be easily localized in the structure using neutrons. Another interesting aspect of neutron diffraction is the possibility to distinguish between neighboring elements like Mn, Co, and Ni, which have essentially similar scattering in X-rays. However the interaction of neutrons with matter, unlike X-rays, is very weak and thus usually a large amount of material is needed for the neutron powder diffraction (NPD) measurements, along with longer data acquisition time. This makes it difficult to design a good and reliable *in situ* NPD cell.

There exist different *in situ* NPD cell designs for battery materials, whether for Li-ion batteries or other battery systems.[3–6] However, in all the published cell designs several drawbacks are apparent. Most of the cell designs result in the presence of many cell parts within the neutron beam, *viz.* counter electrode, separator, both current collectors, cell body, *etc.* This results in appearance of additional undesired Bragg reflections in the diffraction pattern. Moreover, some cell designs use large quantities of electrolyte, which in turn results in higher background intensity and normally in high cost when using deuterated solvents. Thus, recently a rectangular *in situ* NPD cell was designed in our laboratory for use at the High Resolution Powder Diffractometer for Thermal Neutrons (HRPT) beamline at Swiss Spallation Neutron Source (SINQ), PSI Villigen.[7] This cell has an

Paul Scherrer Institut, Electrochemistry Laboratory, CH-5232 Villigen PSI, Switzerland. E-mail: petr.novak@psi.ch; Fax: +41 56 310 4415; Tel: +41 56 310 2457

† Electronic supplementary information (ESI) available. See DOI: 10.1039/c2ra21526h

‡ Present address: Robert Bosch Battery Solutions GmbH, RBDB/ENC, D-70442 Stuttgart, Germany.

§ Present address: CEA Liten, Laboratoire des Matériaux pour les Batteries, F-38054 Grenoble Cedex 9, France.

advantage over the other designs in that only the electrode material soaked with electrolyte and the aluminum or titanium current collector are in the neutron beam. Moreover, by tuning the active material to conductive carbon ratio in the cell, *in situ* NPD patterns with lower background intensities were obtained.[8] Increased amount of carbon additives reduce the ohmic resistance, while increasing the background intensity. Thus an optimum ratio between the active material and the conductive additive is needed as discussed in ref. 8. Nevertheless, this cell design suffered from the large amount of electrode material (~3 g) needed for a good NPD pattern, which drastically affected the electrochemistry of the material.[7,8] Secondly, due to the rectangular design of the previous *in situ* NPD cell, an anisotropic absorption of the diffracted neutron beams could not be avoided, resulting in a challenging full pattern Rietveld refinement of the *in situ* NPD patterns. In order to overcome these drawbacks, a circular *in situ* NPD cell was designed to be used at a high intensity neutron source. In this paper, the proof of concept of this circular cell design has been presented along with the first *in situ* NPD results obtained for $LiFePO_4$ and graphite as model active materials.

Experimental

Cell design and electrochemistry

Fig. 1(A) shows the cross-section view of the new circular *in situ* NPD cell design, whereas Fig. 1(B) shows the position of the cell in the neutron beam. The cell depicted in Fig. 1(A) consists of several parts. The outer cell body (5) is made up of aluminum and is separated from the inner cell body by (6) polyetheretherketone (PEEK). The inner cell body consists of a titanium plunger (2) pushed down from the titanium current collector (4) by a spring (3) to guarantee a homogeneous pressure on the electrode material. The titanium plunger acts as the support for the counter electrode, normally a disk of lithium metal. The sample holder (1) is a thin-walled (0.5 mm) cylinder and is the only part of the cell, besides the porous electrode, that is in the neutron beam during diffraction measurement. This part is 15 mm in diameter and has a height of 3.5 mm. It holds the electrode material and simultaneously acts as the current collector. Ideally, this container would be a metal that is inherently non- or low-scattering in neutrons, *e.g.*, vanadium.[9] Nevertheless, the cost of bulk vanadium is rather high and the machining difficult. Another possibility could be the use of Ti–Zr null matrix alloy.[10] Ti–Zr alloy in atomic ratio 62% : 38% is essentially non-scattering for neutrons. This alloy being commercially unavailable, making and machining a pure Ti–Zr alloy that is non-scattering in a neutron beam is extremely difficult. Therefore, for the development of the *in situ* cell and tests of the new design, aluminum was selected for the sample holder (1) because of its low neutron absorption coefficient and small scattering cross-section. Due to the alloying of aluminum with lithium at low potentials, a titanium container was designed with the same dimensions for cycling of negative electrode materials. O-Rings are used between different parts to seal the cell hermetically. The dimensions of the sample holder for the circular *in situ* NPD cell have been drastically reduced from its rectangular predecessor [53 × 19 × 5.8 mm^3 (l × w × h)], resulting in reduction of the sample holder volume from 5.84 cm^3 to 0.62 cm^3.

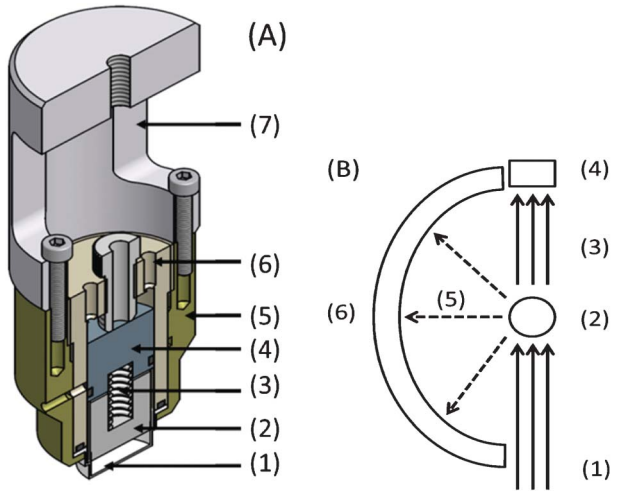

Fig. 1 (A) Cross-section of the new circular *in situ* NPD cell: (1) Al/Ti container for the electrode material (the only part in neutron beam), (2) Ti plunger for Li counter electrode, (3) spring, (4) Ti current collector, (5) Al cell body part, (6) PEEK cell, (7) polymeric attachment for D20 beamline. (B) Top-view schematics showing the position of *in situ* NPD cell (2) in relationship to the incident beam (1) and the detector (6). Out-going beam (3), beam stopper (4), and diffracted beam (5) are also marked.

In order to check the electrochemical performance of different active materials in the circular *in situ* NPD cell, $Li_{1.1}(Ni_{1/3}Mn_{1/3}Co_{1/3})_{0.9}O_2$, carbon-coated $LiFePO_4$, and $Li_4Ti_5O_{12}$ were tested in an aluminum container while graphite was tested in a titanium container. To assemble the cell, the active material and Super-P carbon (TIMCAL, Switzerland) powders were hand mixed in a mortar, and were packed into the container. In case of the graphite no Super-P carbon was used. A glass fiber separator was placed on top of the material and was soaked with either standard protonated ethylene carbonate (EC)/dimethyl carbonate (DMC) 1 M $LiPF_6$ (Ferro, USA) or deuterated ethylene carbonate (d-EC)/dimethyl carbonate (d-DMC) 1 M $LiPF_6$ or deuterated propylene carbonate (d-PC)/dimethyl carbonate (d-DMC) 1 M $LiClO_4$ (Armar AG, Switzerland). A lithium metal disk acted as the counter electrode. The complete cell assembly was performed in an Ar-filled glove box. The $LiFePO_4$, $Li_4Ti_5O_{12}$, and $Li_{1.1}(Ni_{1/3}Mn_{1/3}Co_{1/3})_{0.9}O_2$ cells were cycled at C/24 rate, and the graphite cell at C/200 rate with respect to theoretical specific charge of the active material used. In this study, Li metal and lithium-containing active materials were made up of naturally occurring lithium (mixture of ^6Li and ^7Li) and no isotope-enriched lithium was used.

Ex situ neutron powder diffraction (NPD)

In order to have starting models for quantitative analysis of diffraction patterns obtained using the *in situ* NPD cell using the Rietveld method, *ex situ* NPD measurements were

performed at 1.36 Å for 24 min on dry starting $LiFePO_4$ powder (2 g) and dry $LiFePO_4$ electrode mixture [0.25 g of $LiFePO_4$ (85 wt%) and Super-P carbon (15 wt%)] electrochemically pre-charged till 4.5 V *vs.* Li/Li^+, held in a vanadium cylinder. Rietveld refinement was performed on these patterns using the structural models proposed by Andersson *et al.*[11] For the starting $LiFePO_4$ only a single phase Rietveld refinement was used, whereas for the electrode obtained after the first charge a 2-phase Rietveld refinement with $LiFePO_4$ and $FePO_4$ phases was performed.

Ex situ NPD measurements were then conducted at 1.36 Å for 24 min on the $LiFePO_4$ electrode [0.25 g of $LiFePO_4$ (85 wt%) and Super-P carbon (15 wt%)] in the completely assembled cell, soaked with deuterated propylene carbonate (d-PC)/deuterated dimethyl carbonate (d-DMC) 1 M $LiClO_4$ as the electrolyte. A similar experiment was carried out using an electrochemically pre-charged $LiFePO_4$ porous electrode soaked in deuterated electrolyte. The structural models obtained from Rietveld refinement of dry samples in vanadium cylinders were used for the Rietveld refinement of the patterns from electrolyte-soaked electrodes held in Al containers. Only the zero, scale factor, and the peak width parameters were refined. In both the cases an additional Al phase was introduced to refine the corresponding peaks from the Al container.

In order to differentiate between the quality of NPD pattern obtained using protonated and deuterated electrolyte, a cell was assembled using starting $LiFePO_4$ and Super-P carbon mixture soaked in protonated EC/DMC 1 M $LiClO_4$ electrolyte and *ex situ* NPD pattern was recorded for it at 1.36 Å for 24 min at the D20 beamline.

In situ neutron powder diffraction (NPD)

For the *in situ* NPD measurements, 0.28 g mixture of carbon-coated $LiFePO_4$ (85 wt%) and Super-P carbon (15 wt%) was taken as the electrode mass. No PVDF binder was used to avoid hydrogen in the sample and reduce diffuse scattering from amorphous polymers. The *in situ* cell was assembled as described previously using EC/DMC 1 M $LiClO_4$ electrolyte. For the *in situ* measurements, the cell was charged *versus* Li counter electrode at C/24 rate with respect to 170 mA h g^{-1} till 4.5 V *vs.* Li/Li^+ and then held at open circuit potential (OCP) for 2 h. Due to the limited time allocated at the beamline only the first charge for $LiFePO_4$ was tested, where an *in situ* NPD pattern was recorded during the operation of the cell for a period of 24 min or 0.01667 Li^+ exchange.

In another study *in situ* NPD measurement was performed on graphite, using deuterated electrolyte. For this purpose 0.24 g of SFG44 graphite powder (TIMCAL, Switzerland) was placed in a titanium container. The cell was assembled as described above using deuterated d-EC/d-DMC 1 M $LiPF_6$ (6.8 ppm water) electrolyte. As the aim of this study was to investigate the structural evolution starting from graphite to stage 2 L, the *in situ* NPD patterns were recorded over 30 min at 1.36 Å and 50 °C (±1), only between 0.23 and 0.11 V *vs.* Li/Li^+ [points 1 to 5 in Fig. 2(B)].

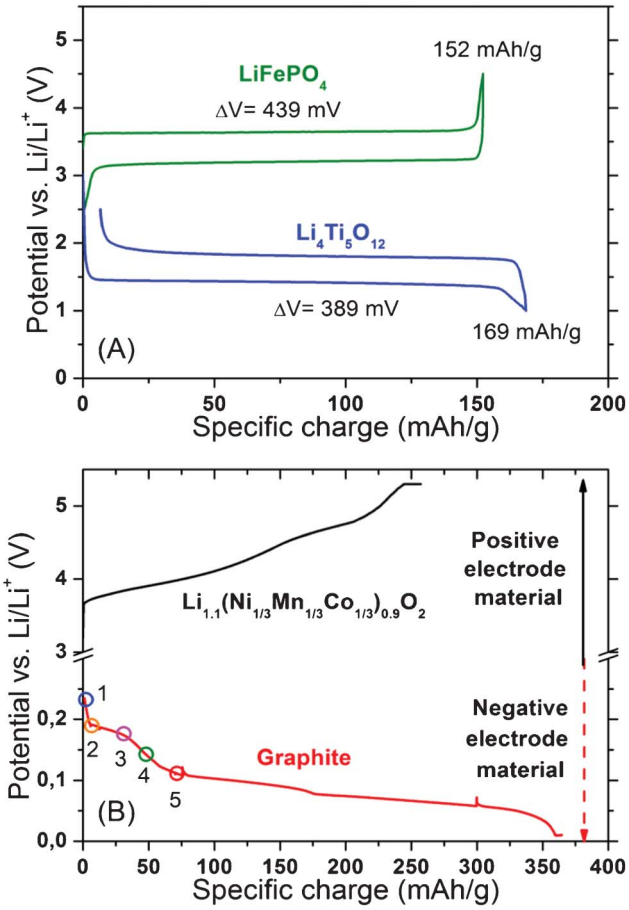

Fig. 2 (A) First electrochemical cycle of $LiFePO_4$ and $Li_4Ti_5O_{12}$, (B) first delithiation and lithiation of $Li_{1.1}(Ni_{1/3}Co_{1/3}Mn_{1/3})_{0.9}O_2$ and graphite, respectively, at different C-rates (indicated in the manuscript) in the circular *in situ* NPD cell *versus* Li counter-electrode. The *in situ* NPD measurements on graphite (Fig. 7) were performed between the points 1 and 5.

Results and discussion

In order to test the feasibility of the circular cell design to cycle various electroactive materials, $Li_{1.1}(Ni_{1/3}Mn_{1/3}Co_{1/3})_{0.9}O_2$, $LiFePO_4$, $Li_4Ti_5O_{12}$, and graphite were cycled in aluminum or titanium containers at different C-rates. In the case of $LiFePO_4$ and $Li_4Ti_5O_{12}$, the internal resistance in the *in situ* cell (seen in Fig. 2(A) as the difference between the lithiation and delithiation curve) is slightly higher when compared to a standard electrochemical cell, which is expected due to the use of ~0.3 g electrode material. In the case of $LiFePO_4$, the overpotential during charge (η_c = 193 mV) was seen to be smaller than that for discharge (η_c = 246 mV). It was reported by Shin *et al.* that at higher C-rates for carbon-coated $LiFePO_4$ phase transition during discharge is difficult compared to charge.[12] A similar effect is also expected for a larger quantity of carbon-coated $LiFePO_4$ cycling at lower C-rates, owing to the higher local surficial current densities. However, despite the higher internal resistance in the *in situ* cell, both the electrode materials deliver ⩾90% of their theoretical specific charge during cycling, with >95% coulombic efficiency during the first cycle. The electrode

composition for $Li_{1.1}(Ni_{1/3}Mn_{1/3}Co_{1/3})_{0.9}O_2$ and graphite electrodes was not optimized and hence only their first delithiation and lithiation are shown, respectively (first electrochemical cycle of these materials in coin-like cells shown in ESI, Fig. A†). As seen from Fig. 2(B), the circular cell can be used over the complete range of interest for the battery materials, *i.e.*, from 0.01 up to 5.2 V *vs.* Li/Li^+ with the same cell design. From these electrochemical results it can be concluded that the circular cell design shows significant improvement over the rectangular predecessor.[7]

Fig. 3 shows the Rietveld refinement method performed on the NPD patterns of the dry $LiFePO_4$ powder and the $LiFePO_4$ electrode after 1st charge, held in a vanadium cylinder. As expected the analysis confirmed that both the starting $LiFePO_4$ and the $FePO_4$ present in the electrode mass at the end of first charge crystallize in the orthorhombic *Pnma* space group. Table 1 and 2 detail the results of the Rietveld analysis. For the $LiFePO_4$ electrode after the 1st charge [Fig. 3(B)], the signal-to-noise ratio is low owing to the fact that the electrode contained 15% carbon, which is a neutron scatterer, that a small amount (0.25 g) of material was used, and that the material has undergone an electrochemical delithiation step. The sloped background made the selection of background points slightly difficult and hence the refinement challenging compared to the starting $LiFePO_4$, where 2 g of sample was used for the measurement. Nonetheless, a Rietveld method could be performed for both the samples over the complete 2 theta range with good fitting. The unit cell parameters and the atomic positions obtained from the Rietveld analysis for $LiFePO_4$ and $FePO_4$ are close to those reported earlier.[13]

These structural models reported in Tables 1 and 2 were then used for the Rietveld refinement of NPD patterns from electrodes in completely assembled cells, soaked with deuterated electrolyte (Fig. 4), where only the zero, the scale factor, and the peak width parameters were refined. In both cases, a small amount of electrode material (0.25 g) was used that contained 15 wt% carbon additive. This resulted in an uneven background of the NPD patterns. Additional high intensity reflections from the Al container are also visible. Thus, the Rietveld refinement to determine correctly the cell parameters and atomic positions is challenging. A Rietveld refinement could be performed by excluding the Bragg reflections from Al. This however also excludes several peaks from the active material overlapping or close to the Al Bragg reflections. As the primary goal of this study was to design and validate an *in situ* cell that allows Rietveld refinement of NPD patterns over the complete 2 theta range, to this point it is recommended to start with a good structural model to avoid large errors during the data interpretation (unless a non-scattering container can be used as the sample holder in the *in situ* NPD cell). In this study, the Rietveld refinement of $LiFePO_4$ NPD pattern after 1st charge showed that 94.5% of $LiFePO_4$ has reacted to form $FePO_4$. This value is close to 90.5% expected from the

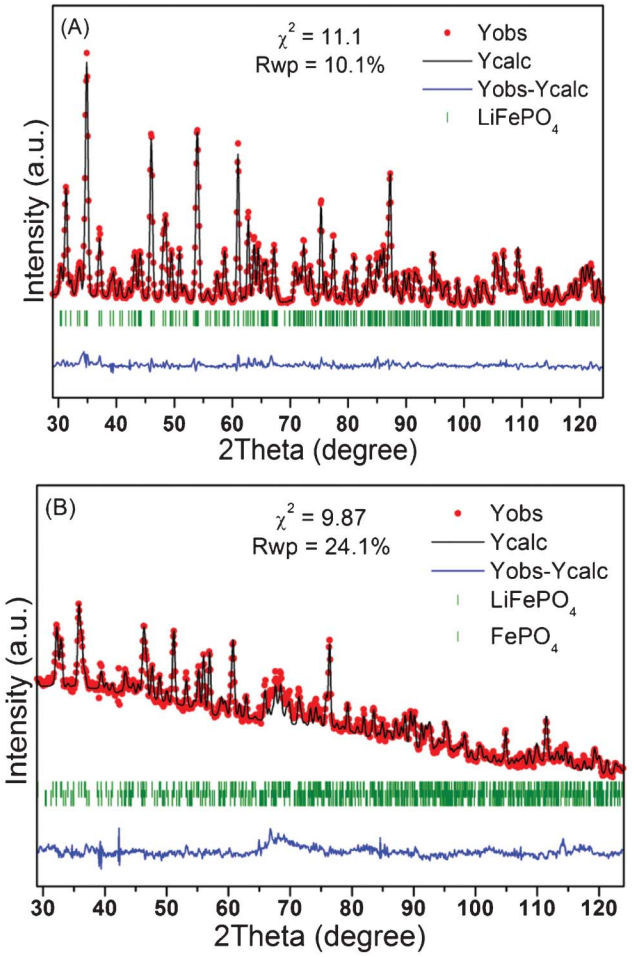

Fig. 3 Rietveld refinement of *ex situ* NPD pattern (λ = 1.36 Å) of (A) dry $LiFePO_4$ pristine powder and (B) dry $LiFePO_4$ electrode mass after 1st charge till 4.5 V *vs.* Li/Li^+. The samples were enclosed in a vanadium cylinder.

Table 1 Crystallographic data obtained from Rietveld analysis of starting $LiFePO_4$ sample. Measurement was performed on dry powder in vanadium cylinder. Refined parameters are in italics

$LiFePO_4$, *Pnma*, a = 10.3279(1) Å, b = 6.0063(1) Å, c = 4.6933(1) Å

Atom	Wyckoff position	x	y	z	B_{iso}	Occupancy
Li	4a	0.0	0.0	0.0	*1.45(16)*	1.0
Fe	4c	*0.2817(2)*	0.25	*0.9753(4)*	*0.685(11)*	1.0
P	4c	*0.0949(3)*	0.25	*0.4163(6)*	*0.685(11)*	1.0
O1	4c	*0.0971(3)*	0.25	*0.7431(6)*	*0.685(11)*	1.0
O2	4c	*0.4566(2)*	0.25	*0.2073(1)*	*0.685(11)*	1.0
O3	8d	*0.1659(1)*	*0.0462(3)*	*0.2836(4)*	*0.696(26)*	1.0

2 theta range/ step increment	0.1°–150.9°/0.1°
Refinement program	Fullprof suite version 2007
Number of measured reflections	489
Zero shift	−0.2769°
Phases and weight percentages	$LiFePO_4$ (100%)
Reliability factors	R_p = 9.39%, R_{wp} = 10.1%, R_{exp} = 3.04%, χ^2 = 11.1, Bragg R-factor = 6.33%

Table 2 Crystallographic data obtained from Rietveld analysis of $LiFePO_4$ electrode after 1st charge till 4.5 V *vs.* Li/Li^+. Measurement was performed on dry electrode mass in vanadium cylinder. Refined parameters are in italics

$FePO_4$, *Pnma*, a = 9.8260(1) Å, b = 5.7941(1) Å, c = 4.7839(1) Å

Atom	Wyckoff position	x	y	z	B_{iso}	Occupancy
Fe	4c	*0.2757(5)*	0.25	*0.9492(10)*	0.495(56)	1.0
P	4c	*0.0925(9)*	0.25	*0.3923(16)*	0.547(59)	1.0
O1	4c	*0.1181(7)*	0.25	*0.7073(14)*	0.547(59)	1.0
O2	4c	*0.4405(7)*	0.25	*0.1619(15)*	0.547(59)	1.0
O3	8d	*0.1668(5)*	*0.0421(9)*	*0.2463(13)*	0.479(54)	1.0

2 theta range/ step increment	0.1°–150.9°/0.1°
Refinement program	Fullprof suite version 2007
Number of measured reflections	455
Zero shift	−0.2745°
Phases and weight percentages	$FePO_4$ (94.5%) and $LiFePO_4$ (5.5%)
Reliability factors	R_p = 23.7%, R_{wp} = 24.1%, R_{exp} = 7.69%, χ^2 = 9.87, Bragg R-factor = 17.1%

electrochemistry. This proves that by using reliable starting structural models a good fitting could be obtained for the NPD patterns recorded using the *in situ* NPD cell.

Fig. 5 compares the NPD patterns recorded for $LiFePO_4$ electrode at open circuit potential in two completely assembled circular *in situ* NPD cells, one with protonated EC/DMC 1 M $LiClO_4$ electrolyte (A) and another with deuterated d-PC/d-DMC 1 M $LiClO_4$ electrolyte (B). It is immediately evident that moving to a protonated electrolyte leads to a higher background intensity in the NPD pattern. Most of the peaks from $LiFePO_4$ that were clearly visible when a deuterated electrolyte was used are no longer detectable. Only the most intense peaks of the electroactive material possess a sufficient signal-to-noise ratio to be detected. Nevertheless, to test the feasibility of using much cheaper protonated electrolyte for *in situ* NPD measurements, the first *in situ* NPD tests with $LiFePO_4$ electrode was performed using protonated EC/DMC 1 M $LiClO_4$. Every sixth *in situ* NPD pattern recorded during the electrochemical operation of the *in situ* cell, corresponding to 10% of specific charge, has been plotted in Fig. 6. It is seen qualitatively from Fig. 6 that during the course of first charge the peaks corresponding to the $LiFePO_4$ phase disappear, while that from $FePO_4$ emerge. When 50% specific charge has been withdrawn from the material, both the phases coexist, proving that evolution of different phases can be followed using the circular *in situ* NPD cell. For the pattern at the end of the first charge, only the intense peaks from the $FePO_4$ are visible. This study on $LiFePO_4$ thus shows that using the inexpensive protonated electrolyte, evolution of the diffraction peaks can be followed qualitatively. However, to obtain well-resolved NPD patterns during electrochemical cycling for quantitative analysis a deuterated electrolyte must be used.

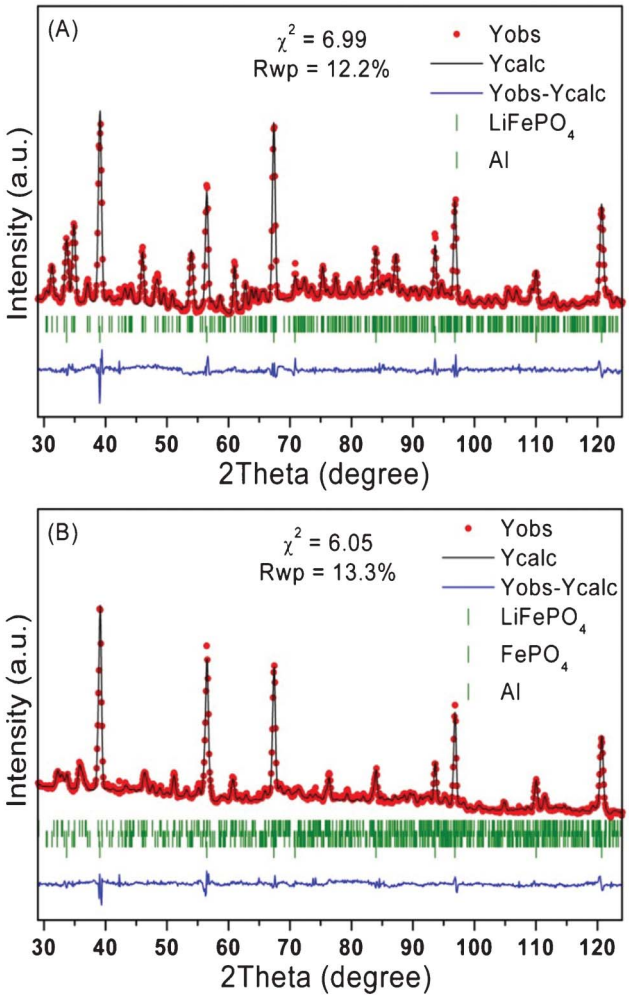

Fig. 4 Rietveld refinement of *ex situ* NPD pattern (λ = 1.36 Å) of (A) $LiFePO_4$ pristine electrode at open circuit potential and (B) $LiFePO_4$ electrode after 1st charge till 4.5 V *vs.* Li/Li^+. The samples were soaked in deuterated d-PC/d-DMC 1 M $LiClO_4$ electrolyte and held in completely assembled circular *in situ* NPD cell in an aluminum container.

Thus, the second *in situ* NPD study of graphite in the circular cell was conducted using deuterated electrolyte. The preliminary data has been presented here with the aim of showing the performance of the circular *in situ* NPD cell when a deuterated electrolyte is used (Fig. 7). The titanium container that was used in order to assist cycling of graphite at potentials negative to 1 V *vs.* Li/Li^+ shows a large number of diffraction peaks due to its hexagonal space group $P6_3/mmc$. However, the major peaks from graphite and titanium do not overlap. From the *in situ* NPD patterns the main (002) peak is seen to shift to lower 2 theta values, *i.e.*, higher c unit cell parameter, which is expected as also shown by Dahn.[14] Several other reflections are seen to evolve during the course of lithiation due to the transition to stage 4 L, 3 L, and 2 L. Owing to the fact that a deuterated electrolyte was used and that graphite itself is a very good neutron scatterer, the signal/noise ratio was sufficiently high. As no proper crystallographic models are

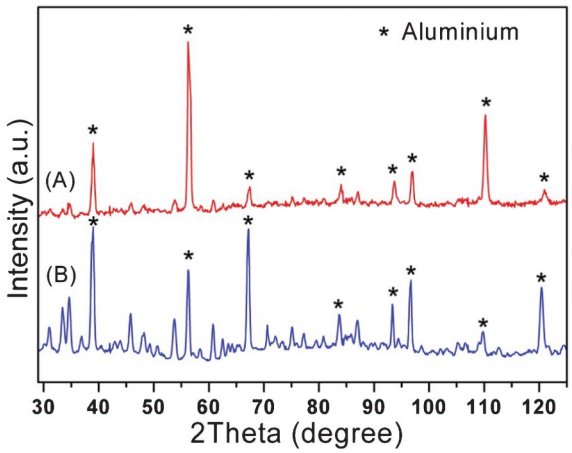

Fig. 5 Comparison of NPD patterns (λ = 1.36 Å) recorded over 24 min for $LiFePO_4$ electrode held in a completely assembled circular *in situ* NPD cell in an aluminum container soaked with (A) protonated EC/DMC 1 M $LiClO_4$ and (B) deuterated d-PC/d-DMC 1 M $LiClO_4$ electrolyte.

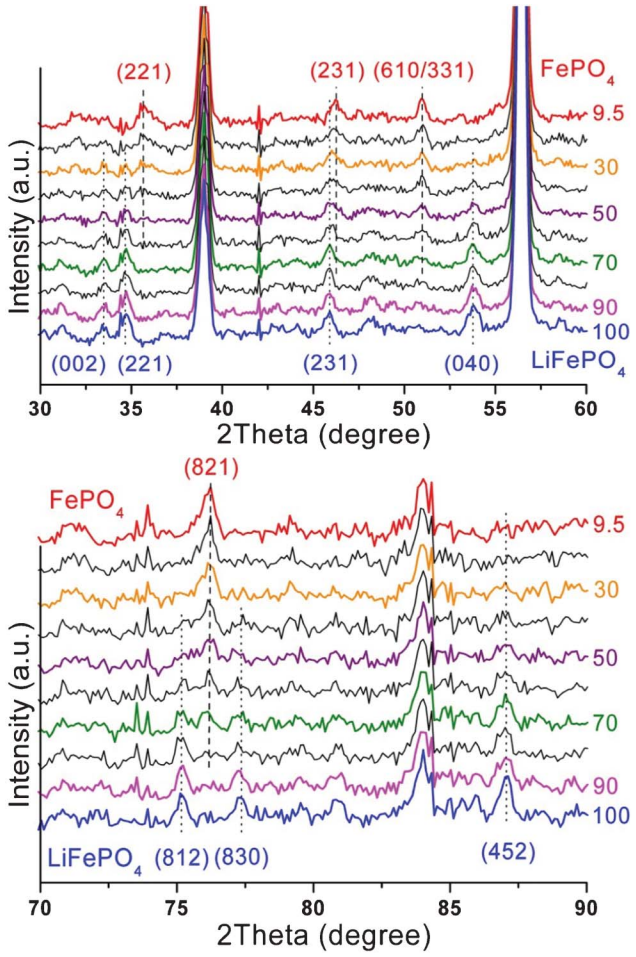

Fig. 6 *In situ* NPD patterns (λ = 1.36 Å) recorded during 1st charge of $LiFePO_4$ till 4.5 V *vs.* Li/Li^+. The numbers on the right-hand side of the patterns represent the nominal percentage of $LiFePO_4$ in the sample as calculated from the electrochemical curve.

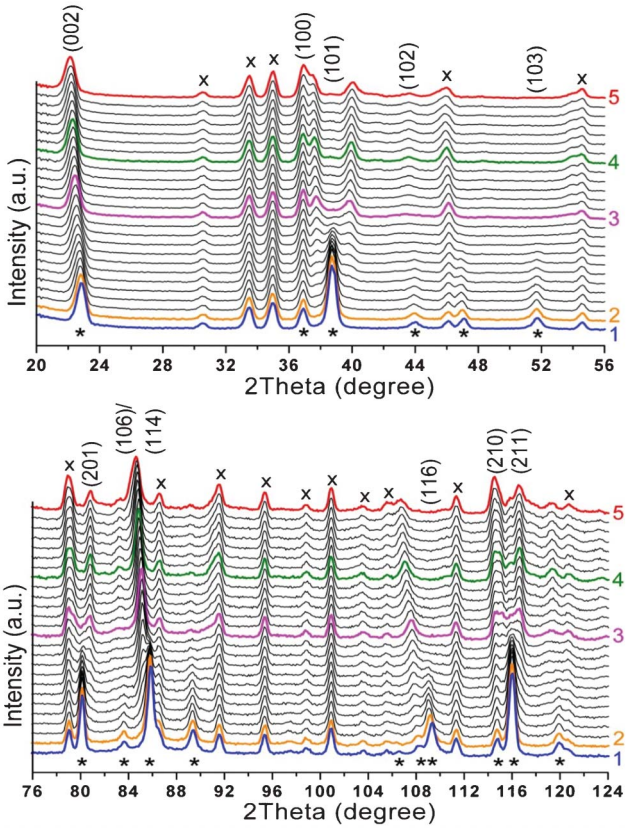

Fig. 7 *In situ* NPD patterns (λ = 1.36 Å) recorded during first lithiation of graphite between 0.23–0.11 V *vs.* Li/Li^+. * and x mark peaks from graphite and titanium, respectively. Major Bragg reflections for graphite are indexed.

available for the different liquid-like stages in graphite, the analysis of the *in situ* NPD data is still ongoing. However, this example clearly illustrates the feasibility of using the new circular *in situ* NPD cell design to follow the structural evolution in electroactive materials for Li-ion batteries in real time.

In summary, from the results it can be concluded that Rietveld refinement method can be performed on NPD data from the electroactive material and carbon mixture, filled in a cylindrical sample holder soaked with deuterated electrolyte. A very good and reliable fitting can be obtained if an acceptable structural model is used. However, when a protonated electrolyte is used instead of a deuterated one, fewer peaks from the sample itself are visible. Moreover, the use of protonated electrolyte leads to an increased background and low signal/background ratio, making it very difficult and unreliable to perform quantitative analysis of the data. Thus, if one intends to perform qualitative and quantitative analysis of the *in situ* NPD data, a pure and dry deuterated electrolyte must be used. Use of protonated electrolyte will only allow for qualitative analysis of evolution of different phases. In terms of electrochemistry the cell was tested for C-rates up to C/10. Cycling at higher rates could be possible but would not be advisable due to challenges with increased electrochemical polarization.

Conclusion

A new *in situ* neutron powder diffraction (NPD) cell based on a circular geometry, capable of cycling 0.2–0.3 g of electrode mass, was designed and successfully tested at the D20 beamline at ILL, Grenoble, France. From the *ex situ* NPD measurements, it was concluded that the use of deuterated electrolyte allows for a qualitative and quantitative analysis of the diffraction patterns. Using this circular cell, the first *in situ* NPD run using $LiFePO_4$ in protonated EC/DMC 1 M $LiPF_6$ electrolyte was successfully conducted at the D20 beamline. As the $LiFePO_4$ was charged at C/24 rate, NPD patterns were recorded over 24 min, *i.e.*, 0.01667 Li^+, making it possible to follow the evolution of different phases qualitatively. The *in situ* NPD experiment performed using graphite soaked in deuterated EC/DMC 1 M $LiPF_6$ electrolyte showed very good electrochemistry and high signal/noise ratio for the NPD patterns. The evolution of several peaks from graphite could be followed qualitatively and analysis is ongoing to identify and quantify the different phases. In conclusion, it can be said that a reliable *in situ* NPD cell cycling a small amount of electroactive material at faster rates and lower data acquisition time has been successfully developed.

Acknowledgements

We thank Dr Thomas Hansen, beamline scientist at the D20 beamline, ILL, Grenoble, for his technical support during the neutron powder diffraction measurements. We are grateful to Dr Tsuyoshi Sasaki and Mr Christoph Junker for their help during the experiments and fruitful discussions. We also thank the Swiss National Science Foundation (SNF) for the funding.

References

1 J.-M. Tarascon and M. Armand, *Nature*, 2001, **414**(6861), 359.
2 Y. Nishi, *Chem. Rec.*, 2001, **1**(5), 406.
3 H. Berg, H. Rundlov and J. O. Thomas, *Solid State Ionics*, 2001, **144**(1–2), 65.
4 O. Bergstrom, A. M. Andersson, K. Edstrom and T. Gustafsson, *J. Appl. Crystallogr.*, 1998, **31**(5), 823.
5 M. A. Rodriguez, D. Ingersoll, S. C. Vogel and D. J. Williams, *Electrochem. Solid-State Lett.*, 2004, **7**(1), A8.
6 N. Sharma, G. Du, A. J. Studer, Z. Guo and V. K. Peterson, *Solid State Ionics*, 2011, **199–200**, 37.
7 F. Rosciano, M. Holzapfel, W. Scheifele and P. Novák, *J. Appl. Crystallogr.*, 2008, **41**, 690.
8 J.-F. Colin, V. Godbole and P. Novák, *Electrochem. Commun.*, 2010, **12**(6), 804.
9 V. F. Sears, *Neutron News*, 1992, **3**(3), 26.
10 A. Boulineau, L. Croguennec, C. Delmas and F. Weill, *Solid State Ionics*, 2010, **180**(40), 1652.
11 A. S. Andersson, B. Kalska, L. Häggström and J. O. Thomas, *Solid State Ionics*, 2000, **130**(1–2), 41.
12 H. C. Shin, K. Y. Chung, W. S. Min, D. J. Byun, H. Jang and B. W. Cho, *Electrochem. Commun.*, 2008, **10**, 536.
13 V. A. Streltsov, E. L. Belokoneva, V. G. Tsirelson and N. K. Hansen, *Acta Crystallographica B*, 1993, **49**(2), 147.
14 J. R. Dahn, *Phys. Rev. B: Condens. Matter*, 1991, **44**(17), 9170.